The International Journal of Advanced Manufacturing Technology (2018) 99:2295–2307
https://doi.org/10.1007/s00170-018-2583-8

ORIGINAL ARTICLE

Position-dependent geometric errors measurement and identification for rotary axis of multi-axis machine tools based on optimization method using double ball bar

Weichao Peng[1] · Hongjian Xia[1] · Xindu Chen[1] · Zeqin Lin[1] · Zhifeng Wang[1] · Haiyan Li[1]

Received: 3 April 2018 / Accepted: 14 August 2018 / Published online: 1 September 2018

Abstract
Geometric errors measurement and identification for rotary table are important. However, precisely adjustment for the setup position of a double ball bar in each measurement pattern is inconvenient. This study proposes a novel optimization identification method using a double ball bar to recognize the position-dependent geometric errors (PDGEs) of rotary axis. A mathematical model for ball bar measurement is firstly constructed to map the relationship between measurement direction and position of the double ball bar. And then, the setup positions of the double ball bar for PDGEs identification are analyzed. According to analysis for setup positions of the double ball bar, simplified measurement patterns would be conducted by adjusting only two setup positions for the ball bar and thus reduce the procedure of accurate adjustment for the ball bar. The PDGEs can be fitted as an nth B-spline curve, on the account of its being smooth and continuous. To identify the PDGEs, an optimization method, by computing the suitable value of control points of nth B-spline curve of errors to minimize the optimal value of the target function between the actual measured value and the value derived from a theoretical measurement model, is proposed. Moreover, in order to obtain the accurate value of control points of the error curve, the sensitivity analysis is conducted to acquire the sensitivity matrix with respect to control points of errors. The PDGEs are able to be identified simultaneously after calculating the appropriate values of control points of errors. The proposed identification method is validated by simulation and experiment. The results prove the effectiveness of the proposed method.

Keywords Geometric errors · Rotary axis · Double ball bar · Multi-axis machine tool · Optimization method · Sensitivity analysis

1 Introduction

A multi-axis machine tool, providing the ability to process parts with complex shapes and high efficiency, is essential in the field of processing industry [1]. The machining precision is essential for multi-axis machine tool. Elements that cause the processing inaccuracy include geometric errors, thermal errors, and servo tracking errors [2]. Considering the non-cutting conditions, the primary error sources are caused by geometric errors [3]. The geometric errors resulting from imperfect assembly can be compensated for the repetitive nature [4]. Therefore, accuracy geometric errors measurement for machine tool is a key issue for improving the machine tools accuracy, especially in ultra-precision occasion.

Geometric errors identification for linear axis is investigated from considerable studies by laser interferometer [5, 6]. However, the geometric errors for multi-axis machine tool are difficult to measure directly because of the existence of rotary axis. In terms of ISO 230-7 [7], position-dependent geometric errors (PDGEs) and position-independent geometric errors (PIGEs) are the two primary error sources for geometric errors of rotary axis. Geometric errors direct measurement for rotary axis is still difficult now [8]. For indirect measurement method, it is feasible to separate errors from measurement results by a precise instrument. Several indirect methods with a double ball bar [9–17], laser interferometer tracker [18, 19], tough trigger probe [20, 21], and *R*-test [22]

Electronic supplementary material The online version of this article (https://doi.org/10.1007/s00170-018-2583-8) contains supplementary material, which is available to authorized users.

✉ Hongjian Xia
hjxia@gdut.edu.cn

[1] Guangdong Provincial Key Laboratory of Micro-nano Manufacturing Technology and Equipment, School of Electromechanical Engineering, Guangdong University of Technology, Guangzhou 510006, Guangdong, China

are proposed recently. The double ball bar, which convenient to place on rotary axis without accessory equipment, is a suitable instrument for geometric errors measurement for rotary axis by the control of linear axes simultaneously.

During the past decades, considerable researches have been taken to geometric errors measurement and identification for rotary axis by double ball bar. Zhu [4] presented an identification method to recognize the geometric errors of rotary axis for five-axis machine tool by a double ball bar. The test was applied with the ball bar that is motionless relative to the rotary axis reference coordinate when the axis rotates. Three measurement positions of ball bar would be needed during the test. Jiang [23] proposed an identification method for the PIGEs of rotary axis by the ball bar. During the whole measurement, the ball set on the workbench without disassembly and the measurements were applied with or without extension bar to isolate errors from other axes. Lee [24] proposed a method to recognize the PIGEs of rotary axis with two measurement paths. Chen [25] presented a method to recognize the PDGEs and PIGEs of rotary table with a tilt table by two steps. To identify the PDGEs, the ball bar is adjusted to three different directions in turn. In each ball bar measurement position, the precisely adjustment procedure would be needed. Lasemi [10] presented an identification method with double ball bar for geometric errors of rotary axis by three-axis controlled motions. A very large number of measurement points are required to be measured for geometric errors identification of rotary axis. Xiang [26] use ball bar to identify five PDGEs of each rotary ax by five patterns. The PDGEs were measured in sensitivity direction of double ball bar in each pattern and a number of disassembly for double ball bar was conducted. Fu [27] proposed a six-circle identification method based on differential motion matrix. Six measurement patterns in three different setup positions are implemented and each pattern is required to measure in the sensitivity direction of double ball bar. A decoupled method was proposed to identify geometric errors of rotary axis [28]. However, the method required several measurement patterns and every pattern needs accurately adjustment for double ball bar.

From the above researches, troublesome adjustment for the double ball bar would be needed. In order to propose a convenient identification method, this paper decreases the measurement positions of double ball bar so as to decrease troublesome adjustment for the double ball bar. The minimum setup positions of double ball bar for recognition of six PDGEs are investigated and B-spline curve of errors are used for reducing the number of measuring points in each measurement pattern. According to the previous researches, it is more complicated to identify PDGEs rather than PIGEs for rotary axis [8]. The approach that identifies PIGEs of rotary axis is relatively mature [23, 24] and the method, which identifies PDGEs of rotary axis, needs more setup and measurement points of double ball bar or simultaneous control of axes motion. In addition, numerous disassembly and setup positions of double ball bar would cause more setup errors and thus affect the identified result of geometric errors. Precisely adjusting double ball bar in each measurement pattern is also troublesome. Moreover, the aforementioned studies mainly concerned about the machine configuration with a tilting or rotary table. For those configurations, the identification procedure can be simplified for setting the ball bar at the reference coordinate origin of rotary axis. For the configuration with a tilting head, little research has been done.

This paper proposed a novel identification method with double ball bar to recognize the PDGEs of rotary axis on machine configuration with a tilting head. A mathematical model based on kinematic analysis is applied to deduce the relationship between measurement direction and position of double ball bar. In order to reduce the procedure of accurate adjustment for double ball bar, only two setup positions would be implemented and three measuring paths on each setup position of double ball bar would be applied during the measurement. The angular errors and displacement errors would be considered as an nth B-spline curve for its being smooth and continuous. The value of these errors would be determined by the control points of the nth B-spline curve. The PDGEs of rotary axis is identified by calculating the appropriate value of the control points of nth B-spline curves of errors, which minimize the target value of the objective function between the actual measured value and the value derived from the theoretical measurement model. Furthermore, sensitivity matrix with respect to control points of errors was derived from sensitivity analysis so as to acquire the more accurate control points.

The structure of this paper is as follows. Section 2 described the detail for kinematic model of rotary axis. The identification method for the PDGEs of rotary axis and the optimization method are discussed in Section 3. In Section 4, the simulation and experiment are conducted and their results are discussed. Finally, the contribution of this article is given in Section 5.

2 Kinematic analysis of rotary axis

2.1 Geometric error of rotary axis

According to the ISO 230-7, the PDGEs consist of three displacement errors and three angular errors. Their value changes when the table rotates. The displacement errors and angular errors of PDGEs are represented as symbol $\delta_i(j)$ and $\varepsilon_i(j)$, respectively. The direction of error is represented by subscript. The character in brackets represents the motion axis. Taking rotational axis B as an example, these symbols are shown in Fig. 1 and written as Table. 1. As Fig. 2 shows, a commonly used machine tool with a tilting head is taken to validate the proposed method. On the workbench side, the rotational axis B is set on the linear axis Z and rotates around Y direction. On

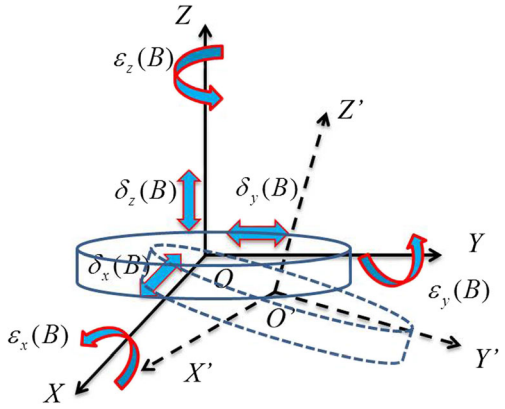

Fig. 1 The PDGEs of rotary axis

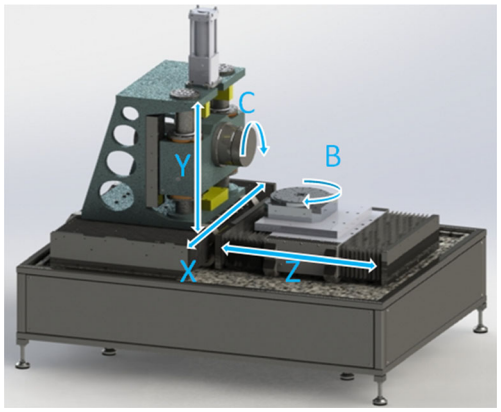

Fig. 2 Configuration of multi-axis machine tool

the spindle side, a rotational axis *C* is equipped on the linear axis *Y*. The linear axis *Y* is installed on the linear axis *X*.

2.2 Kinematic model

According to the kinematic theory [28, 29], the relationships between the kinematic pair are shown in Fig. 3. As the method that identify PIGEs of rotary axis is relatively mature to be measured and compensated, assume the PIGEs of rotary axis has been compensated. Based on the position B_i, the origin of body B_{i+1}connected with B_i can be expressed as

$$r_{i+1} = r_i + s_{i(i+1)} + \varepsilon_{i(i+1)} \tag{1}$$

where r_i is the position vector in the direction from the reference frame $(O_0X_0Y_0Z_0)$ to the reference frame of B_i $(O_iX_iY_iZ_i)$. $S_{i(i+1)}$ is the constant vector in the direction from the reference frame $(O_iX_iY_iZ_i)$ to the reference frame$(O_i^bX_i^bY_i^bZ_i^b)$,and $\varepsilon_{i(i+1)}$ is the position error vector.

The orientation transformation matrix of B_{i+1}could be expressed as

$$A_{i+1} = A_iC'_{i(i+1)}A'_{i(i+1)}A''_{i(i+1)} \tag{2}$$

where A_i is the transformation matrix of B_i $(O_iX_iY_iZ_i)$ relative to the reference frame $(O_0X_0Y_0Z_0)$ and $C'_{i(i+1)}$ is the transformation matrix of the frame $(O_i^bX_i^bY_i^bZ_i^b)$ relative to the reference frame $(O_iX_iY_iZ_i)$.

Table 1 The notations of PDGEs of rotary axis B

Axis B	Displacement errors			Angular errors		
	X	Y	Z	X	Y	Z
PDGEs	$\delta_x(\beta)$	$\delta_y(\beta)$	$\delta_z(\beta)$	$\varepsilon_x(\beta)$	$\varepsilon_y(\beta)$	$\varepsilon_z(\beta)$

The origin of body B_{i+1}can be expressed as follows:

$$r_{i+1} = r_i + A_i\left(S'_{i(i+1)} + C'_{i(i+1)}\left(A'_{i(i+1)}\varepsilon'_{i(i+1)}\right)\right) \tag{3}$$

Taking rotational axis *B* as an example, the transformation matrixes can be expressed as

$$A'_{i(i+1)} = \begin{bmatrix} \cos(\beta) & 0 & \sin(\beta) \\ 0 & 1 & 0 \\ -\sin(\beta) & 0 & \cos(\beta) \end{bmatrix}, A''_{i(i+1)} = \begin{bmatrix} 1 & -\varepsilon_z(\beta) & \varepsilon_y(\beta) \\ \varepsilon_z(\beta) & 1 & -\varepsilon_x(\beta) \\ -\varepsilon_y(\beta) & \varepsilon_x(\beta) & 1 \end{bmatrix}$$
$$, \varepsilon'_{i(i+1)} = \begin{bmatrix} \delta_x(\beta) \\ \delta_y(\beta) \\ \delta_z(\beta) \end{bmatrix} \tag{4}$$

The detailed derivation procedure can be found in Reference [28]. In comparison with the homogeneous transformation matrices method [30], the modeling based on kinematic theory has the advantage: it provides explicit relationship between the errors and the motion of kinematic bodies.

2.3 Double ball-bar measurement

In a practical application of ball bars, one ball is set on spindle, and the other ball is placed on the workbench, shown in Fig. 4. The geometric errors cause the deviation from ideal position for the ball on the workbench. The ball bar fixed on the spindle is also affected by the geometric errors of linear axes. Fortunately, the errors of linear axes can be measured and compensated directly [4]. Thus, for the spindle side, the error of the ball can be eliminated. In this article, as the methods that identify PIGEs of rotary axis are relatively mature to be measured and compensated, assume that the PIGEs of rotary axis have been compensated. Therefore, only the PDGEs of rotary axis cause the measurement deviation for double ball bar. According to the kinematic method [28], the deviation between two balls can be represented by

$$\Phi^{dist} = (r_w - r_t)^T(r_w - r_t) - R^2 \tag{5}$$

where r_w is the central position of the ball on the workbench. r_t

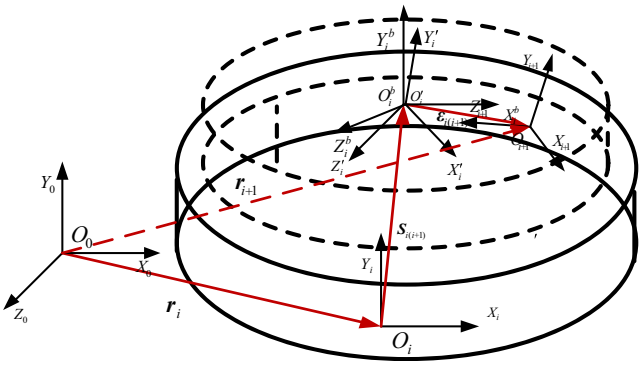

Fig. 3 Kinematic notations of rotary axis

is the central position of the ball on the spindle. R represents the ideal ball bar length.

Based on the kinematic model, r_w and r_t can be deduced as

$$r_w = r_b + A_b A'_{bw}\left(\varepsilon'_{bw} + A''_{bw} r'_p\right) \tag{6}$$

$$r_t = r_b + A_b A'_{bw}\left(r'_p + S'_R\right) \tag{7}$$

where $r'_p = [P_x \;\; P_y \;\; P_z]^T$ is the position vector between the origin of the reference frame ($O_i^b X_i^b Y_i^b Z_i^b$) and central position of the ball on the workbench. $S'_R = [R_x \;\; R_y \;\; R_z]^T$ is the direction vector between two balls.

Because the errors of rotary axis are very small, ignore the high-order deviations. Putting Eqs. (4), (6)–(7) into Eq. (5), the distance can be written as

$$\Phi^{dist} = 2\begin{bmatrix} R_x \\ R_y \\ R_z \end{bmatrix}^T \begin{bmatrix} 0 & -P_z & P_y \\ P_z & 0 & P_x \\ -P_y & P_x & 0 \end{bmatrix} \begin{bmatrix} \varepsilon_x(\beta) \\ \varepsilon_y(\beta) \\ \varepsilon_z(\beta) \end{bmatrix} - 2\begin{bmatrix} R_x \\ R_y \\ R_z \end{bmatrix}^T \begin{bmatrix} \delta_x(\beta) \\ \delta_y(\beta) \\ \delta_z(\beta) \end{bmatrix} \tag{8}$$

Assume that ΔR is the ball bar variation distance. Neglecting the high-order deviations for it is relatively small.

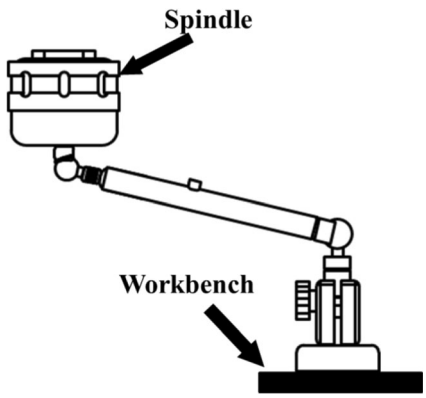

Fig. 4 Installation of double ball bar

According to Reference [28], the variation distance for the double ball bar are represented as

$$\Phi^{dist} = (R + \Delta R)^2 - R^2 = 2R\Delta R + \Delta R^2 = 2R\Delta R \tag{9}$$

According to the Eqs. (8)–(9), the ball bar measurement variation caused by geometric errors are deduced

$$R\Delta R = \begin{bmatrix} R_x \\ R_y \\ R_z \end{bmatrix}^T \begin{bmatrix} 0 & -P_z & P_y \\ P_z & 0 & P_x \\ -P_y & P_x & 0 \end{bmatrix} \begin{bmatrix} \varepsilon_x(\beta) \\ \varepsilon_y(\beta) \\ \varepsilon_z(\beta) \end{bmatrix} - \begin{bmatrix} R_x \\ R_y \\ R_z \end{bmatrix}^T \begin{bmatrix} \delta_x(\beta) \\ \delta_y(\beta) \\ \delta_z(\beta) \end{bmatrix} \tag{10}$$

Eq. (10) can be simplified as

$$R\Delta R(\beta) = [-\bar{P}R - R]\begin{bmatrix} \varepsilon(\beta) \\ \delta(\beta) \end{bmatrix} \tag{11}$$

where $P = [P_x \;\; P_y \;\; P_z]^T$ is the position vector between the origin of the reference frame ($O_i^b X_i^b Y_i^b Z_i^b$) and the central position of the ball on the workbench. $R = [R_x \;\; R_y \;\; R_z]^T$ is the direction vector between two balls. The symbol $\bar{P}$ represents the function $P\times$. The operator '×' performs the cross product. $\varepsilon(\beta)$ is the angular errors of rotary axis B. $\delta(\beta)$ is the displacement errors of rotary axis B.where $\varepsilon(\beta) = [\varepsilon_x(\beta) \;\; \varepsilon_y(\beta) \;\; \varepsilon_z(\beta)]$ and $\delta(\beta) = [\delta_x(\beta) \;\; \delta_y(\beta) \;\; \delta_z(\beta)]$.

3 Identification of PDGEs of rotary axis

The PDGEs consist of three displacement errors and three angular errors. Their value changes when the table rotates. Some researchers applied method, which require three or more setup procedures for double ball bar and two or more measurement patterns in each setup position, for the identification of six PDGEs simultaneously. It is inconvenient to precisely adjust the setup procedures for ball bar in each measurement pattern. For reducing the troublesome adjustment, the minimum ball bar setup positions for recognition of six PDGEs are investigated. The geometric errors are modeled by the nth B-spline curve, which has the characteristic of local control, which is contributed only in the range between the first and last of specific knots and is zero elsewhere. By this means, limited control points of errors are measured to determine the curve shape of errors rather than measure the whole range of rotary axis. In addition, three measurement paths on each setup position of double ball bar would be conducted, which ensure each error of PDGEs contributes to the effect of measurement deviation of double ball bar in each measurement range. Moreover, a boundaryless constraint optimization algorithm was applied to calculate the control points of errors

through the discrete measurement data and thus recognize the six PDGEs of rotary axis.

3.1 Analysis of setup positions of double ball bar

Because the geometric errors are unavoidable, there is deviation between the real position of the ball on the workbench and the ideal position. Theoretically speaking, moving the ball bar in the position P_1 ($[P_{1x} \quad P_{1y} \quad P_{1z}]$) by the spindle to three different direction R_1 ($[R_{1x} \quad R_{1y} \quad R_{1z}]$), R_2 ($[R_{2x} \quad R_{2y} \quad R_{2z}]$) and R_3 ($[R_{3x} \quad R_{3y} \quad R_{3z}]$), the variation distance ΔR ($[\Delta R_1 \ \Delta R_2 \ \Delta R_3]$) can be acquired from the ballbar test software. From Eq. (11), it can be simplified as

$$R\Delta R = R\begin{bmatrix}\Delta R_1\\ \Delta R_2\\ \Delta R_3\end{bmatrix} = \begin{bmatrix}-\bar{P}_1R_1-R_1\\ -\bar{P}_1R_2-R_2\\ -\bar{P}_1R_3-R_3\end{bmatrix}\begin{bmatrix}\varepsilon(\beta)\\ \delta(\beta)\end{bmatrix} \tag{12}$$

In order to let Eq. (12) have the unique solution, according to linear algebra theory [31], there exit three coefficients (κ_1, $\kappa_2$and κ_3). Only when they are all equal to zero ($\kappa_1 = 0$, $\kappa_2 = 0$ and κ_3 = ;0), Eq.(13) is workable. It can be simplified as

$$\kappa_1[-\bar{P}_1R_1-R_1] + \kappa_2[-\bar{P}_1R_2-R_2] + \kappa_3[-\bar{P}_1R_3-R_3] = 0 \tag{13}$$

where κ_1, κ_2,and κ_3 are corresponding parameters. Obviously, if the three directions (R_1, R_2, R_3) of double ball bar are non-linear correlation relative to each other, the coefficient matrix in Eq. (12) would be nonsingular. Thus three non-linear correlation directions (R_1, R_2, R_3) exit making the solution in Eq. (12) unique.

Then, adjust the position of the ball, on the workbench, to the position P_2 ($[P_{2x} \quad P_{2y} \quad P_{2z}]$) and moving the ball bar by the spindle to two different directions (R_4, R_5), the variation ΔR (ΔR_4, ΔR_5) can be acquired. From Eq. (11), it can be simplified as

$$R\Delta R = R\begin{bmatrix}\Delta R_1\\ \Delta R_2\\ \Delta R_3\\ \Delta R_4\\ \Delta R_5\end{bmatrix} = \begin{bmatrix}-\bar{P}_1R_1-R_1\\ -\bar{P}_1R_2-R_2\\ -\bar{P}_1R_3-R_3\\ -\bar{P}_2R_4-R_4\\ -\bar{P}_2R_5-R_5\end{bmatrix}\begin{bmatrix}\varepsilon(\beta)\\ \delta(\beta)\end{bmatrix} \tag{14}$$

In order to let Eq. (14) have the unique solution, according to the above theory, there exit five coefficients (κ_1, κ_2, κ_3, κ_4,and κ_5) . Only when they are all equal to zero, Eq. (15) is workable. It can be simplified as.

$$\begin{aligned}&\kappa_1\left[-\bar{P}_1R_1-R_1\right] + \kappa_2\left[-\bar{P}_1R_2-R_2\right] + \kappa_3\left[-\bar{P}_1R_3-R_3\right]\\ &+\kappa_4\left[-\bar{P}_2R_4-R_4\right] + \kappa_5\left[-\bar{P}_2R_5-R_5\right] = 0\end{aligned} \tag{15}$$

With multiple P_1 on both sides of Eq. (15), it can be expressed as

$$\begin{aligned}&\kappa_1\left[-P_1\bar{P}_1R_1-P_1R_1\right] + \kappa_2\left[-P_1\bar{P}_1R_2-P_1R_2\right] + \kappa_3\left[-P_1\bar{P}_1R_3-P_1R_3\right]\\ &+\kappa_4\left[-P_1\bar{P}_2R_4-P_1R_4\right] + \kappa_5\left[-P_1\bar{P}_2R_5-P_1R_5\right] = 0\end{aligned}$$

Table 2 Measurement patterns for PDGEs of rotary axis B

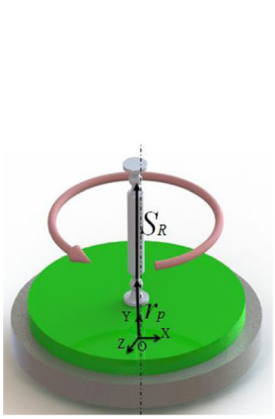

1st measurement pattern

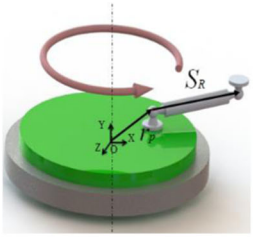

2nd measurement pattern

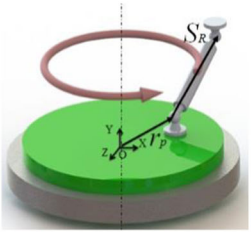

3rd measurement pattern

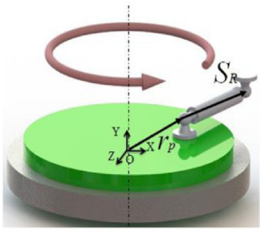

4th measurement pattern

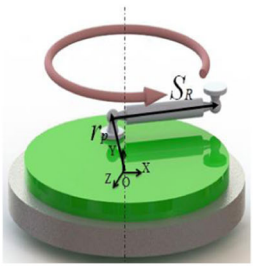

5th measurement pattern

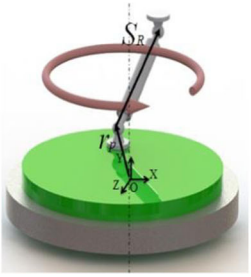

6th measurement pattern

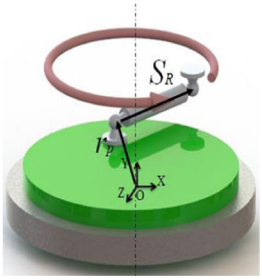

7th measurement pattern

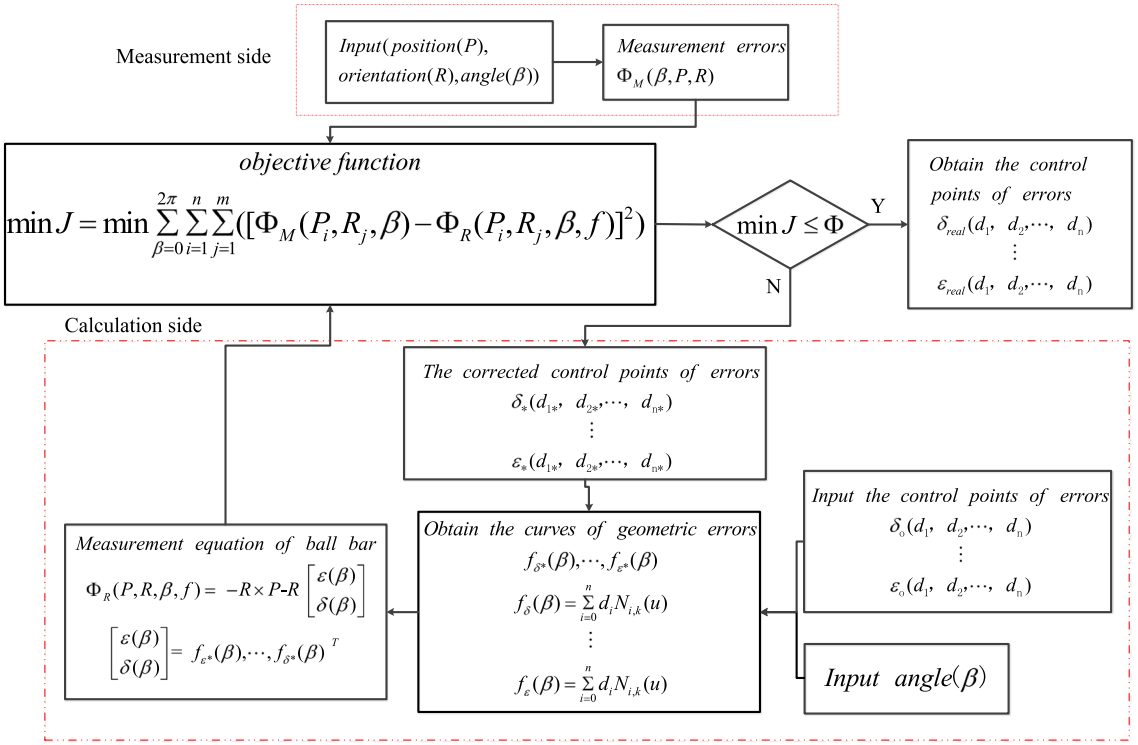

Fig. 5 Flowchart of identification of PDGEs of rotary axis

It is obviously, $P_1\bar{P}_1 = 0$, then

$$\kappa_1[0-P_1R_1]+\kappa_2[0-P_1R_2]+\kappa_3[0-P_1R_3]+\kappa_4\left[-P_1\bar{P}_2R_4-P_1R_4\right] +\kappa_5\left[-P_1\bar{P}_2R_5-P_1R_5\right]=0 \tag{16}$$

According to the Eq. (16), if the $(-(P_1\bar{P}_2(\kappa_4R_4+\kappa_5R_5))\neq 0)$, Only when they are all equal to zero ($\kappa_1=0$, $\kappa_2=0$, $\kappa_3=0$, $\kappa_4=0$, $\kappa_5=0$), Eq.(16) is workable. Obviously, it is easily to find two non-linear correlation directions (ΔR_4, ΔR_5) of the double ball bar to make the formula $(P_1\bar{P}_2(\kappa_4R_4+\kappa_5R_5))$ not equal to zero and not parallel to P_2 and P_1 if five coefficients (κ_1, κ_2, κ_3, κ_4,and κ_5) are not equal to zero together.

Finally, moving the ball bar by the spindle to one additional direction ($R6$), the variation ΔR (ΔR_6) can be obtained. From Eq. (11), it can be simplified as

$$R\Delta R = R\begin{bmatrix}\Delta R_1\\ \Delta R_2\\ \Delta R_3\\ \Delta R_4\\ \Delta R_5\\ \Delta R_6\end{bmatrix} = \begin{bmatrix}-\bar{P}_1R_1-R_1\\ -\bar{P}_1R_2-R_2\\ -\bar{P}_1R_3-R_3\\ -\bar{P}_2R_4-R_4\\ -\bar{P}_2R_5-R_5\\ -\bar{P}_2R_6-R_6\end{bmatrix}\begin{bmatrix}\varepsilon(\beta)\\ \delta(\beta)\end{bmatrix} \tag{17}$$

Firstly, the three direction (ΔR_4, ΔR_5,and ΔR_6) of double ball bar should be a non-linear correlation relative to each other to ensure the formula ($\left[-\bar{P}_2R_4-R_4\ -\bar{P}_2R_5-R_5\ -\bar{P}_2R_6-R_6\right]$) is nonsingular. In order to let Eq. (17) have the unique solution, according to the above theory, there exit six coefficients (κ_1, κ_2, κ_3, κ_4, κ_5, and κ_6), Only when they are all equal to zero, Eq.(18) is workable. It can be simplified as.

$$\kappa_1\left[-\bar{P}_1R_1-R_1\right]+\kappa_2\left[-\bar{P}_1R_2-R_2\right]+\kappa_3\left[-\bar{P}_1R_3-R_3\right] +\kappa_4\left[-\bar{P}_2R_4-R_4\right]+\kappa_5\left[-\bar{P}_2R_5-R_5\right]+\kappa_6\left[-\bar{P}_2R_6-R_6\right]=0 \tag{18}$$

Multiple P_1 on both sides of Eq. (18), it can be expressed as

$$\kappa_1[0-P_1R_1]+\kappa_2[0-P_1R_2]+\kappa_3[0-P_1R_3]+\kappa_4\left[-P_1\bar{P}_2R_4-P_1R_4\right] +\kappa_5\left[-P_1\bar{P}_2R_5-P_1R_5\right]+\kappa_6\left[-P_1\bar{P}_2R_6-P_1R_6\right]=0 \tag{19}$$

According to Eq. (19), if the $(-(P_1\bar{P}_2(\kappa_4R_4+\kappa_5R_5+\kappa_6R_6))\neq 0)$, only when they are all equal to zero ($\kappa_1=0$, $\kappa_2=0$, $\kappa_3=0$, $\kappa_4=0$, $\kappa_5=0$,

Table 3 The measurement parameters for double ball bar in measurement patterns (mm)

Patterns	1st	2nd	3rd	4th
Position	(0, 40,0)	(0, 40,-15)	(0, 40,-15)	(0, 40,-15)
Direction	(0,100, 0)	(94.8,0,31.6)	(70.7,70.7,0)	(0,70.7,70.7)
Patterns	5th	6th	7th	8th
Position	(− 15, 40,0)	(− 15, 40,0)	(− 15, 40,0)	(− 20, 80,80)
Direction	(94.8,0,31.6)	(70.7,70.7,0)	(0,70.7,70.7)	(43.3,75,50)

Table 4 The parameters for modeling of PDGEs

PDGEs	$\delta_i(j)$	$\varepsilon_i(j)$
Number of control points	7	6
Order	4	4

and $\kappa_6 = 0$), the Eq. (19) is workable. However, because the three directions (ΔR_4, ΔR_5, and ΔR_6) are nonlinear correlations relative to each other, there are always exits ($\kappa_4 \neq 0$, $\kappa_5 \neq 0$and$\kappa_6 \neq 0$) to make the formula ($\kappa_4 R_4 + \kappa_5 R_5 + \kappa_6 R_6$) parallel to the position vector in the direction from the origin to the position P_2 so as to make the formula $(-(P_1\bar{P}_2(\kappa_4 R_4 + \kappa_5 R_5 + \kappa_6 R_6)) = 0)$. Thus, Eq. (17) is a singular matrix and does not have a unique solution for geometric errors.

From Eq. (14), the five geometric errors in PDGEs can be recognized in two setup procedures for double ball bar. According to Eq. (17), six PDGEs of a rotary axis could not be identified in only two setup positions. Fortunately, the displacement error $\delta_y(\beta)$ is easily measured and compensated. The ball bar direction, which perpendicular to the workbench, is in accordance with the error $\delta_y(\beta)$. Thus, separate displacement error $\delta_y(\beta)$ from other PDGEs of a rotary axis and then measure and compensate it. For doing that, the rest of the five PDGEs can be identified in only two setup positions.

3.2 Measurement path of double ball bar

An effective method is performed for PDGEs identification with only two setup positions. The measurement procedures are shown in Table 2.

In the first measurement pattern, place the ball on the rotation center of workbench, and set the ball bar direction $S_R' = [0 \quad R \quad 0]^T$ and choose setup position $r_p' = [0 \quad P_{y1} \quad 0]^T$ on rotary table. Substitute those parameters into Eq. (11); the equation is deduced below

$$R\Delta R(\beta) = -\begin{bmatrix} 0 \\ R \\ 0 \end{bmatrix}^T \begin{bmatrix} \delta_x(\beta) \\ \delta_y(\beta) \\ \delta_z(\beta) \end{bmatrix} \tag{20}$$

According to Eq. (20), the direction of the ball bar is in accordance with the error $\delta_y(\beta)$ without the influence of the other errors in PDGEs, substituting Eq. (20) into Eq. (10) to deduce the variation $R\Delta R(\beta)$.Thus, the error $\delta_y(\beta)$ is expressed as

$$\delta_y(\beta) = -\Delta R(\beta)$$

In order to identify the rest of the PDGEs, three measurement directions derived from a space spherical helix motion path on each measurement setup position of double ball bar are conducted. The space spherical helix formula is expressed as follows

$$S_R = \begin{bmatrix} S_x \\ S_y \\ S_z \end{bmatrix} = \begin{bmatrix} Rsin(0.5\beta_s)\cos(n\beta_s) \\ Rsin(0.5\beta_s)\sin(n\beta_s) \\ Rcos(0.5\beta_s) \end{bmatrix} \tag{21}$$

where R is the radius of the measurement path, n is the number of helical line, β_s is the rotation angle of spherical helix. S_x, S_y, and S_z are the vector components in the x, y, and z directions of the ball bar, respectively.

The measurement procedures contain four steps and are listed as follows.

(a) The 2nd measurement pattern is selected. Adjust the position of ball, which is located on the workbench, to the position $r_{p1} = [H \quad P_{y1} \quad 0]^T$ and moving the ball by the spindle to the direction $S_{R1} = [S_{x1} \quad S_{y1} \quad S_{z1}]^T$. When the rotary table rotates, keep the ball bar stationary

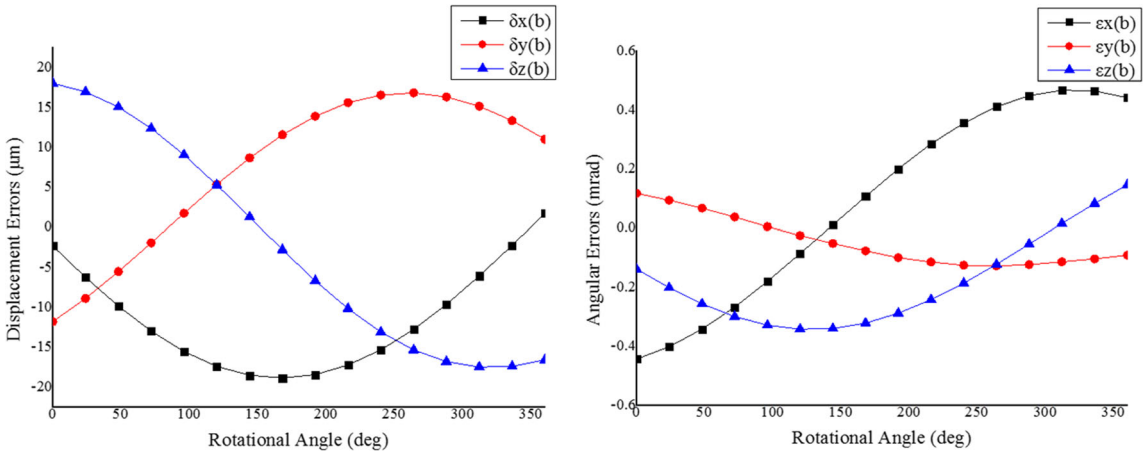

Fig. 6 The generated displacement errors and angular errors of rotary axis

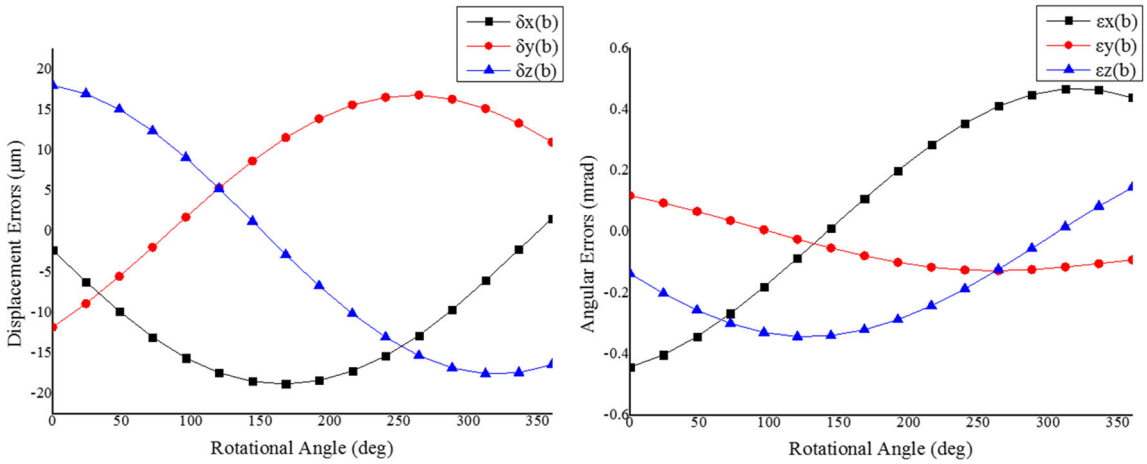

Fig. 7 The identified displacement errors and angular errors of rotary axis

relative to the rotary axis coordinate system and record the deviation of the ball bar. The full process will be repeated until the measurement procedure is finished.

(b) As the 3rd measurement pattern shows, the rotary table and linear axes move synchronously to change the direction of the ball bar to $S_{R2} = [S_{x2} \quad S_{y2} \quad S_{z2}]^T$. It stops to record the deviation of the ball bar at each measurement angle during the measurement until the measurement is finished.

(c) Then, the direction of the ball bar are adjusted to $S_{R3} = [S_{x3} \quad S_{y3} \quad S_{z3}]^T$ by the simultaneous movement of the rotary table and linear axes. As shown in the 4th measurement pattern, it stops to record the deviation of the ball bar. The full process will be repeated until the measurement is completed.

(d) Finally, the ball bar has been adjusted to the mounting position ($r_{p2} = [0 \quad P_{y1} \quad H]^T$), and the ball bar is not disassembled from the socket during the whole measurement. Other measurement procedures (5th, 6th, and 7th measurement patterns) will be executed as the above measurement procedures. Thus, there are six measurement values of the rotary table, which is enough to the solution for five geometric errors.

The identification models consist of the six measurement results and the six geometric errors from Eq. (11).

$$R\Delta R = R\begin{bmatrix}\Delta R_1\\ \Delta R_2\\ \Delta R_3\\ \Delta R_4\\ \Delta R_5\\ \Delta R_6\end{bmatrix} = \begin{bmatrix}-\bar{r}_{p1}S_{R1}-S_{R1}\\ -\bar{r}_{p1}S_{R2}-S_{R2}\\ -\bar{r}_{p1}S_{R3}-S_{R3}\\ -\bar{r}_{p2}S_{R1}-S_{R1}\\ -\bar{r}_{p2}S_{R2}-S_{R2}\\ -\bar{r}_{p2}S_{R3}-S_{R3}\end{bmatrix}\begin{bmatrix}\varepsilon(\beta)\\ \delta(\beta)\end{bmatrix} \tag{22}$$

The displacement error $\delta_y(\beta)$ in PDGEs has been identified before the above measurement procedures. The rank of coefficient matrix of Eq. (22) must be equal to 5 to ensure the solution for Eq. (22). And, the setup parameter H should satisfy the condition ($H \neq 0$). The measurement results of

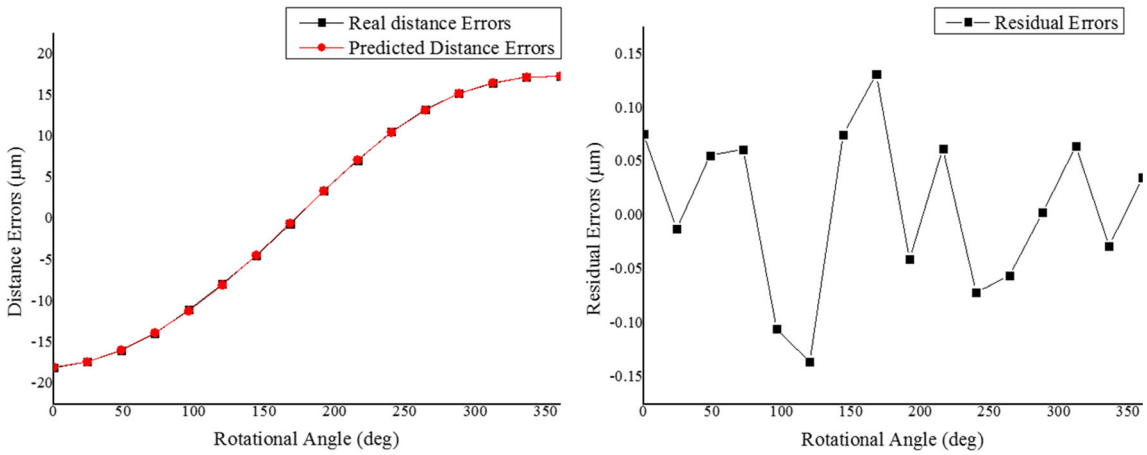

Fig. 8 Comparison results of real distance errors and predicted ones and residual errors

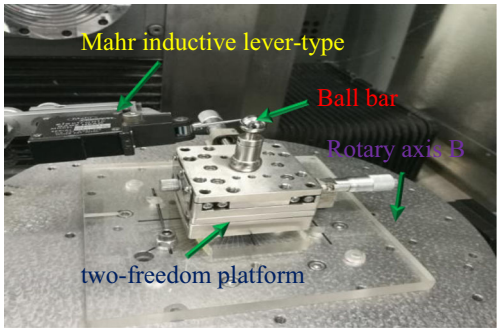

Fig. 9 Setup error correction for double ball bar by lever-type probe

displacement error $\delta_y(\beta)$ are put in Eq. (22), and thus, the rest of the five PDGEs can be identified simultaneously.

3.3 Parametric modeling of PDGEs

For angular errors and displacement errors are generally smooth, continuous, and repeatable, some researchers applied the polynomials to model geometric errors based on discrete measurement results [5, 32, 33]. As it is commonly used in numerical fitting, nth B-spline curve has the characteristic of local control to change the curve shape, which is contributed only in the range between the first and the last of specific knots and is zero elsewhere. And thus, some false measurement points have little influence for the fitting curve of geometric errors, and limited control points of errors are needed to be measured to determine the curve shape of errors rather than measure the whole range of rotary axis. The nth B-spline models for these errors are represented as follows

$$\delta_*(\beta) = \sum_{i=0}^{n} d_i N_{\delta_* i,k}(u)$$

where $d_i$represents the control point and $N_{\delta_* i,k}(u)$ is the basis function for specific error δ_*. The subscript i represents the sequence number and the second subscript k is the order.

Generally speaking, the control point determines the curve shape of errors if the suitable number of control points and order are chosen. To further determine the values of the control points of errors, a method based on optimization method is presented.

3.4 Identification based on optimization method and sensitivity analysis

According to Eq. (11), the measurement deviation data of the ball bar caused by the geometric errors of rotary axis is represented as $\Phi_R(\beta)$. During the actual measurement test, the measurement value in the ball bar measurement system can be represented by $\Phi_M(\beta)$. Therefore, the objective function can be deduced:

$$J = (\Phi_M(\beta) - \Phi_R(\beta))^2$$

where objective function J represents the square deviation between the value of actual measurement and the value derived from the kinematic theory.

Obviously, $\Phi_M(\beta)$ is the measurement value. So, the value of objective function J is related to the identified results of geometric errors. If the identified results of geometric errors are close to the measurement value, the value of $\Phi_R(\beta)$ would be close to the $\Phi_M(\beta)$, and thus, the objective function J would be close to zero. Then, the optimization task is represented by

$$\min J = \min \sum_{\beta=0}^{2\pi} [\Phi_M(\beta) - \Phi_R(\beta)]^2 \Big|_{\delta,\varepsilon} \tag{23}$$

As is well known, optimization method is widely used in engineering application. In this paper, a boundaryless constraint optimization algorithm has been applied to calculate the value of geometric errors. However, the boundaryless constraint optimization algorithm needs a troublesome iterative procedure, and it is easy to calculate the inaccuracy results for the control points of PDGEs and thus result in failure of identification, if the search direction is not restricted and confirmed. For the accurate value of control points of errors and improving the efficiency of the optimization algorithm, the sensitivity analysis is adopted to acquire the

Table 5 The measurement parameters for double ball bar in measurement patterns (mm)

Patterns	1st	2nd	3rd	4th
Position	(0, 83.4,0)	(5, 83.4,0)	(5, 83.4,0)	(5, 83.4,0)
Direction	(2.6,4.5, 99.8)	(2.6,4.5, 99.8)	(27.2,47.2,83.9)	(89.1,0,45.4)
Patterns	5th	6th	7th	8th
Position	(0, 83.4,5)	(0, 83.4,5)	(0, 83.4,5)	(0, 83.4,3)
Direction	(2.6,4.5, 99.8)	(27.2,47.2,83.9)	(89.1,0,45.4)	(80.9,0,58.8)

matrix with respect to control points of PDGEs to confirm the search direction.

Substituting Eq. (23) into Eq. (11), the measurement variation of the ball bar with respect to the corresponding variation of control point of PDGEs can be gotten as

$$\begin{aligned} {\partial J}/{\partial d_\delta} &= \left[{\partial J}/{\partial d_{\delta_x}} \;\; {\partial J}/{\partial d_{\delta_y}} \;\; {\partial J}/{\partial d_{\delta_z}} \;\; {\partial J}/{\partial d_{\varepsilon_x}} \;\; {\partial J}/{\partial d_{\varepsilon_y}} \;\; {\partial J}/{\partial d_{\varepsilon_z}} \right]^T \\ &= 2(\,\Phi_M(\beta) - \,\Phi_R(\beta))\sum_{i=0}^{n} \begin{bmatrix} R_x N_{\delta_x i,k}(u) \\ R_y N_{\delta_y i,k}(u) \\ R_z N_{\delta_z i,k}(u) \\ -(R_y P_z - R_z P_y) N_{\varepsilon_x i,k}(u) \\ -(R_z P_x - R_x P_z) N_{\varepsilon_y i,k}(u) \\ -(R_x P_y - R_y P_x) N_{\varepsilon_z i,k}(u) \end{bmatrix} \end{aligned} \quad (24)$$

where $[P_x \quad P_y \quad P_z]^T$ is the position vector between the origin of the reference frame ($O_i^b X_i^b Y_i^b Z_i^b$) and the central position of the ball on the workbench. $[R_x \quad R_y \quad R_z]^T$ is the direction vector between two balls. $N_{\delta * i,k}(u)$ is the basis function of the corresponding PDGEs (δ_*).

From the above equation, obviously, in order to recognize the PDGEs of rotary axis from the error measurements results, it needs the measurement procedures containing all the impact of PDGEs. The parameters of the coefficient matrix in Eq. (24) have to satisfy the conditions ($R_x \neq 0$, $R_y \neq 0$, $R_z \neq 0$, $(R_y P_z - R_z P_y) \neq 0$, $(R_z P_x - R_x P_z) \neq 0$, and $(R_x P_y - R_y P_x) \neq 0$) in one of the measurement patterns in Table 2. The basis function of the corresponding PDGEs is confirmed if the suitable number of control points and order are chosen. Thus, measurement variation of the ball bar with respect to the corresponding variation of control point of PDGEs can be calculated when recording the measurement points.

A boundaryless constraint optimization algorithm is applied to calculate the control points of nth B-spline curves of geometric errors and a program has been developed to evaluate the value of objective function J changing with the value of geometric errors control point of rotary axis at different rotation angles.

As shown in Fig. 5, the calculation procedures are listed as follows.

On the measurement side, the geometric errors of rotary axis have been measured in terms of the above measurement patterns using double ball bar in the whole workspace. The deviation $\Phi_M(\beta)$ of the ball bar would be recorded from software. The position (P) of the ball cup on the workbench, orientation (R) of the ball bar and the rotation angle (β) of the axis B are recorded during the measurement.

On the calculation side, input a series of corresponding initial points (d_1, d_2, ⋯, d_n), which are represented by the values of control points of nth B-spline curves of PDGEs. Thus, geometric errors would be confirmed through B-spline function ($f_{\delta *}(\beta)$, ⋯, $f_{\varepsilon *}(\beta)$). And then, the theoretical value

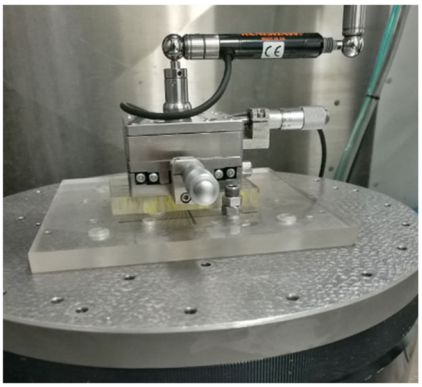

Fig. 10 The 2nd measurement process

($\Phi_R(\beta)$) derived from Eq. (11) would be calculated through the measurement equation of the ball bar.

The theoretical value ($\Phi_R(\beta)$) and the deviation($\Phi_M(\beta)$) of ball bar would be put into the objective function (J). If the value of objective function did not satisfy the conditions ($J \leq \Phi$ (The error tolerance)), the corrected control points (d_{1*}, d_{2*}, ⋯, d_{n*}) of errors derived from sensitivity analysis would be put into the objective function through the above procedure. Finally, there is an optimum values of control points of geometric errors to satisfy the conditions ($J \leq \Phi$) through iterative algorithm, which is called boundaryless constraint optimization algorithm, and corresponding measurement data. Thus, all of the PDGEs (δ_{real}, ε_{real}) are identified by calculating the corresponding control point of nth B-spline curve of geometric errors.

4 Simulation and experiment

4.1 Simulation

To test the effectiveness of the proposed identification method, a simulation is performed for the rotary axis B on the machine configuration with a tilting head (shown in Fig. 2).

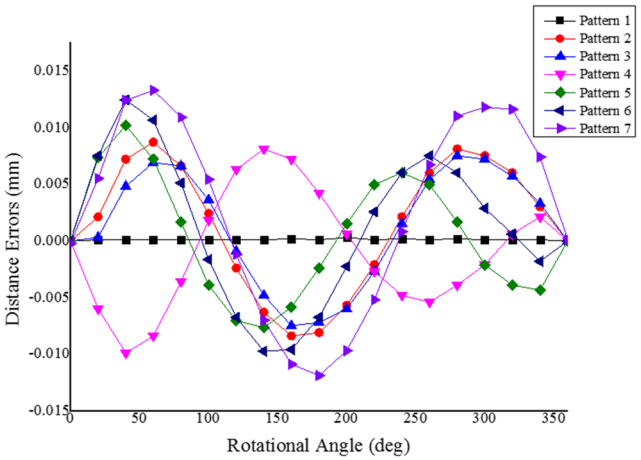

Fig. 11 Measurement results of the measurement patterns

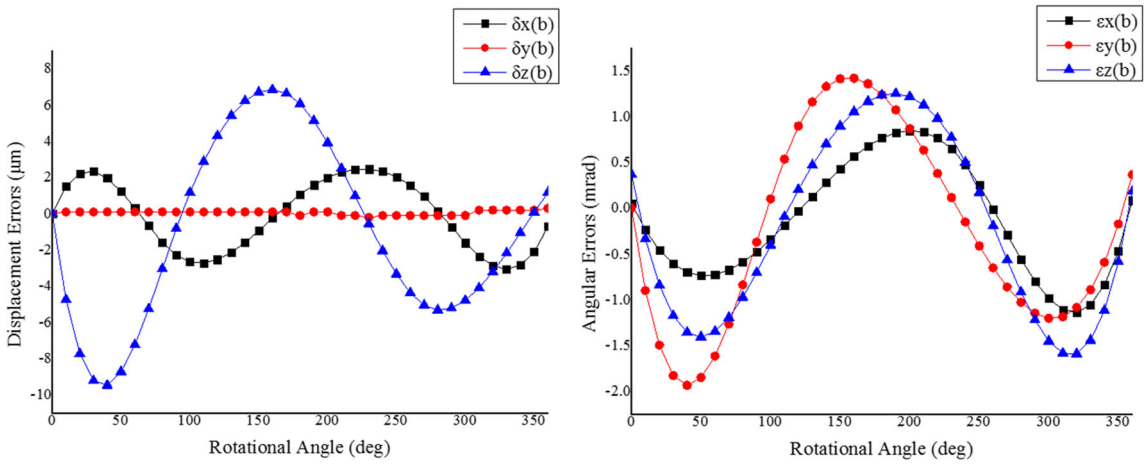

Fig. 12 The identified displacement errors and angular errors of rotary axis

The measurement patterns of the simulation are shown in Table 2. Assuming that the geometric errors of linear axis and the PIGEs of rotary axis have been compensated, those errors are given as zero. Table 3 shows the measurement parameters for the double ball bar in measurement patterns, respectively. The number of control points and order for each geometric error are shown in Table. 4. Figure 6 shows the generated six PDGEs of rotary axis.

The displacement error $\varepsilon_y(\beta)$ of PDGEs is firstly identified by the 1st measurement patterns in Table 2. Then, the identification results of displacement error $\varepsilon_y(\beta)$ are put into Eq. (11). According to the measurement procedure in Section 3, the rest of the identification patterns are taken to identify the rest of the PDGEs. Finally, the measurement results are all put in Eq. (23) and the corresponding sensitivity analysis are performed to identify the PDGEs. The identification results of PDGEs are shown in Fig. 7. To further verify the geometric errors identification method for rotary axis, a comparison simulation is performed to estimate the ball bar variation. Based on the results of generated errors and calculated errors, the measurement results are compared by the 8th pattern. The distance errors are measured at every 20°. Figure 8 shows the residual error between the generated error and the predicted one. For the residual error of rotary axis *B*, the maximum deviation is 0.15 μm. Referring to the results of the simulation, the effectiveness of the proposed method is verified.

4.2 Experiment

The proposed method has been carried out on a Nanotech 350FG type machine tool, whose configuration is shown in Fig. 2. A double ball bar (QC10, Renishaw) with a 100-mm length bar is adopted for the PDGEs measurement of rotary axis *B* in the designed test paths. The working range of machine tool is 350 mm × 150 mm × 300 mm. Before the identification tests, the geometric errors of linear axis and PIGEs of rotary axis are compensated and eliminated by the software-compensated method.

The installation errors of ball are unavoidable for the misalignment between its axis and the spindle. For eliminating the initial setup errors, a Mahr inductive lever-type probe is applied for the adjustment of ball bar. In Fig. 9, the probe is get close to contact the surface of a reference ball. Then, rotate the rotary table and adjust the micrometer on the two-freedom

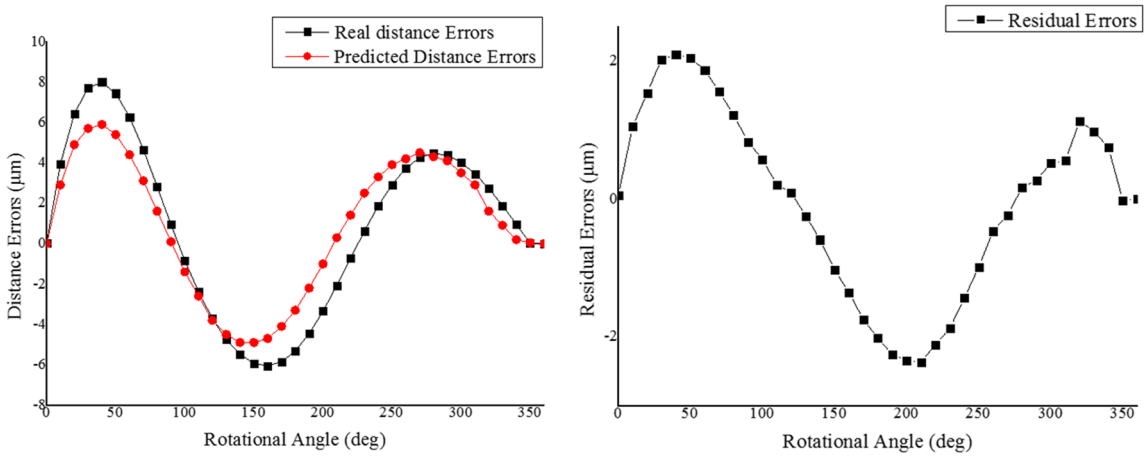

Fig. 13 Comparison results real distance errors and predicted ones and residual errors

movement platform to ensure the axis of ball bar is in accordance with the axis line of the rotary table. The procedures are repeated, ensuring the deviation is within 1 μm from the probe. In addition, in order to let the movement of the micrometer fit in with the coordinate of the machine tool, the probe is used to parallel one side of the platform to the movement of axis *Z* by slightly rotating the rotary table. Finally, the setup error can be eliminated.

In each measurement pattern, the distance between the two balls are kept constant. However, due to the geometric errors exits, the reading from ball bar should be changed during the test. Before the test, the geometric errors of linear axes and PIGEs of the rotary table have been compensated. Thus, the deviation in measurement results can be considered a result from PDGEs. For the PDGEs identification of the rotary table, the proposed identification patterns are implemented. The number and order of control points for each geometric error are shown in Table 4. Table 5 shows the measurement parameters for the double ball bar in measurement patterns. The detailed 2nd measurement processes are shown in Fig. 10. During the test, the deviation errors are measured at every 20° and thus acquire 18 measurement results in each design pattern. Compared to the published method [28], which needs 36 measurement results in each design pattern, the method proposed in this article increase the efficiency of measurement of PDGEs. Fig. 11 shows the results of the measurement patterns.

The identification results of PDGEs are shown in Fig. 12. Based on the results of measured errors and identified errors, the measurement results are compared by the 8th pattern. The distance errors are measured at every 20°. The residual error between the measurement error and the predicted one is shown in Fig. 13. In Fig. 13, the absolute distance error between the maximum and minimum is 14.1 μm. The maximum deviation of the residual error of rotary axis *B* between the measured value and the predicted one is 2 μm. The measurement patterns were conducted in about 100-mm-diameter circular paths. The accuracy of double ball bar is about ± 1 μm. There are also exit errors in the spindle although using the lever-type probe. The maximum deviation (2 μm) is close to the limitation accuracy of double ball bar. Therefore, the method developed in this study can effectively recognize these PDGEs of rotary axis and is possible for precision detection in machine configuration with a tilting head.

5 Conclusion

This paper presented an optimization method using the double ball bar for PDGEs identification of rotary axis. A mathematical model based on kinematic theory is constructed to map the relationship between measurement direction and position of the double ball bar. According to the kinematic model, the PDGEs of rotary axis are able to be identified by selecting suitable setup positions and directions of the ball bar. For reducing the troublesome setup procedures for the double ball bar, the minimum setup positions of the double ball bar are investigated for identification of six PDGEs. According to the kinematic model and the linear algebra theory, since the displacement error $\delta_y(\beta)$ is easily measured and compensated, the other five PDGEs are identified in only two setup positions. In addition, geometric errors are able to be considered as an nth B-spline curve on the account of its being smooth and continuous. As an nth B-spline curve has the characteristic of local control, limited control points of errors are able to be calculated to determine the curve shape of errors rather than measure the whole range of rotary axis so as to simply measure the procedure. To further determine the control points of errors, a method based on the optimization method is presented. A boundaryless constraint optimization algorithm is applied to calculate the control points of geometric errors through iterative procedure. Moreover, In order to acquire accurate values of control points of errors and improve efficiency of the optimization algorithm, the sensitivity analysis is performed to confirm the search direction. Therefore, the PDGEs are able to be identified simultaneously after calculating the appropriate values of control points of errors. Furthermore, the position of the ball bar is accurately adjusted by a micrometer resolution movement platform, and thus, the ball on the workbench is not disassembled during the whole measurement. Finally, simulation and experiment are performed to testify the identification method. According to the results of simulation and experiment, it demonstrates that the effectiveness and accuracy of proposed method.

Acknowledgements The authors would like to express their sincere thanks to the support of the National Natural Science Foundation of China (No.51775116), the Open Operation of Guangdong Provincial Key Laboratory of Micro-nano Manufacturing Technology and Equipment (No. 2017B030314178), and the Guangdong Science and Technology Planning Project (No. 2015B010102011, No. 2015B090921007 and No. 2016B090911001).

References

1. Qiao Y, Chen Y, Yang J, Chen B (2017) A five-axis geometric errors calibration model based on the common perpendicular line (CPL) transformation using the product of exponentials (POE) formula. Int J Mach Tools Manuf 118–119:49–60
2. Ramesh R, Mannan MA, Poo AN (2000) Error compensation in machine tools — a review: part I: geometric, cutting-force induced and fixture-dependent errors. Int J Mach Tool Manu 40(9):1235–1256
3. Schwenke H, Knapp W, Haitjema H, Weckenmann A, Schmitt R, Delbressine F (2008) Geometric error measurement and compensation of machines—an update. CIRP Ann Manuf Technol 57(2): 660–675

4. Zhu S, Ding G, Qin S, Lei J, Zhuang L, Yan K (2012) Integrated geometric error modeling, identification and compensation of CNC machine tools. Int J Mach Tool Manu 52(1):24–29
5. Chen G, Yuan J, Ni J (2001) A displacement measurement approach for machine geometric error assessment. Int J Mach Tool Manu 41(1):149–161
6. Peng W, Xia H, Wang S, Chen X (2017) Measurement and identification of geometric errors of translational axis based on sensitivity analysis for ultra-precision machine tools. Int J Adv Manuf Technol 94(5–8):2905–2917
7. ISO 230-7-2006, Test Code for Machine Tools-Part 7: Geometric Accuracy of Axes of Rotation (2006). ISO
8. Chen JX, Lin SW, Zhou XL, Gu TQ (2016) A ballbar test for measurement and identification the comprehensive error of tilt table. Int J Mach Tool Manu 103:1–12
9. Xiang S, Altintas Y (2016) Modeling and compensation of volumetric errors for five-axis machine tools. Int J Mach Tool Manu 101:65–78
10. Lasemi A, Xue D, Gu P (2016) Accurate identification and compensation of geometric errors of 5-axis CNC machine tools using double ball bar. Meas Sci Technol 27(5):055004
11. Yang J, Ding H (2016) A new position independent geometric errors identification model of five-axis serial machine tools based on differential motion matrices. Int J Mach Tool Manu 104:68–77
12. Tsutsumi M, Tone S, Kato N, Sato R (2013) Enhancement of geometric accuracy of five-axis machining centers based on identification and compensation of geometric deviations. Int J Mach Tool Manu 68(68):11–20
13. Lee DM, Zhu Z, Lee KI, Yang SH (2011) Identification and measurement of geometric errors for a five-axis machine tool with a tilting head using a double ball-bar. Int J Precis Eng Manuf 12(2): 337–343
14. Lee KI, Yang SH (2016) Compensation of position-independent and position-dependent geometric errors in the rotary axes of five-axis machine tools with a tilting rotary table. Int J Adv Manuf Technol 85(5–8):1677–1685
15. Tsutsumi M, Saito A (2003) Identification and compensation of systematic deviations particular to 5-axis machining centers. Int J Mach Tool Manu 43(8):771–780
16. Tsutsumi M, Saito A (2004) Identification of angular and positional deviations inherent to 5-axis machining centers with a tilting-rotary table by simultaneous four-axis control movements. Int J Mach Tool Manu 44(12–13):1333–1342
17. Ibaraki S, Knapp W (2012) Indirect measurement of volumetric accuracy for three-axis and five-axis machine tools: A review
18. Zhang Z, Hu H (2013) A general strategy for geometric error identification of multi-axis machine tools based on point measurement. Int J Adv Manuf Technol 69(5–8):1483–1497
19. Li H, Guo J, Deng Y, Wang J, He X (2016) Identification of geometric deviations inherent to multi-axis machine tools based on the pose measurement principle. Meas Technol 27(12)
20. Jiang Z, Bao S, Zhou X, Tang X, Zheng S (2015) Identification of location errors by a touch-trigger probe on five-axis machine tools with a tilting head. Int J Adv Manuf Technol 81(1–4):149–158
21. Jiang Z, Song B, Zhou X, Tang X, Zheng S (2015) Single setup identification of component errors for rotary axes on five-axis machine tools based on pre-layout of target points and shift of measuring reference. Int J Mach Tool Manu 98(4/5):1–11
22. Ibaraki S, Oyama C, Otsubo H (2011) Construction of an error map of rotary axes on a five-axis machining center by static R-test. Int J Mach Tool Manu 51(3):190–200
23. Jiang X, Cripps RJ (2015) A method of testing position independent geometric errors in rotary axes of a five-axis machine tool using a double ball bar. Int J Mach Tool Manu 89:151–158
24. Lee KI, Yang SH (2013) Measurement and verification of position-independent geometric errors of a five-axis machine tool using a double ball-bar. Int J Mach Tool Manu 70(4):45–52
25. Chen JX, Lin SW, He BW (2014) Geometric error measurement and identification for rotary table of multi-axis machine tool using double ballbar. Int J Mach Tool Manu 77(77):47–55
26. Xiang S, Yang J (2014) Using a double ball bar to measure 10 position-dependent geometric errors for rotary axes on five-axis machine tools. Int J Adv Manuf Technol 75(1–4):559–572
27. Fu G, Fu J, Xu Y, Chen Z, Lai J (2015) Accuracy enhancement of five-axis machine tool based on differential motion matrix: geometric error modeling, identification and compensation. Int J Mach Tool Manu 89:170–181
28. Xia HJ, Peng WC, Ouyang XB, Chen XD, Wang SJ, Chen X (2017) Identification of geometric errors of rotary axis on multi-axis machine tool based on kinematic analysis method using double ball bar. Int J Mach Tool Manu 122:161–175
29. Haug EJ (1989) Computer-Aided Kinematics and Dynamics of Mechanical Systems Volume-I Basic Methods Allyn 1
30. Kong LB, Cheung CF, To S, Lee WB, Du JJ, Zhang ZJ (2008) A kinematics and experimental analysis of form error compensation in ultra-precision machining. Int J Mach Tool Manu 48(12–13):1408–1419
31. Nering ED, Henney DR (1970) Linear algebra and matrix theory. Wiley
32. Fu G, Fu J, Shen H, Sha J, Xu Y (2016) Numerical solution of simultaneous equations based geometric error compensation for CNC machine tools with workpiece model reconstruction. Int J Adv Manuf Technol 86(5–8):2265–2278
33. Fu G, Fu J, Shen H, Yao X, Chen Z (2015) NC codes optimization for geometric error compensation of five-axis machine tools with one novel mathematical model. Int J Adv Manuf Technol 80(9–12): 1879–1894